TECHNICAL NOTE:

Higher-order statistical moments and a procedure that detects potentially anomalous years as two alternative methods describing alterations in continuous environmental data

Running head: long-term changes in environmental data

Ivan Arismendi[1*], Sherri L. Johnson[2] & Jason B. Dunham[3]

[1]Department of Fisheries and Wildlife, Oregon State University, Corvallis, Oregon 97331, USA.

[2]US Forest Service, Pacific Northwest Research Station, Corvallis, Oregon 97331, USA.

[3]US Geological Survey, Forest and Rangeland Ecosystem Science Center, Corvallis, Oregon 97331, USA.

*Corresponding author: Ivan.Arismendi@oregonstate.edu; Phone: (1) 541-750-7443; Fax: (1) 541-758-7760;

Abstract

Statistics of central tendency and dispersion may not capture relevant or desired characteristics of the distribution of continuous phenomena and thus, they may not adequately describe temporal patterns of change. Here, we present two methodological approaches that can help to identify temporal changes in environmental regimes**.** First, we use higher-order statistical moments (skewness and kurtosis) to examine potential changes of empirical distributions at decadal extents. Second, we adapt a statistical procedure combining a non-metric multidimensional scaling technique and higher density region plots to detect potentially anomalous years. We illustrate the use of these approaches by examining long-term stream temperature data from minimally and highly human-influenced streams. In particular, we contrast predictions about thermal regime responses to changing climates and human-related water uses. Using these methods, we effectively diagnose years with unusual thermal variability and patterns in variability through time, as well as spatial variability linked to regional and local factors that influence stream temperature. Our findings highlight the complexity of responses of thermal regimes of streams and reveal their differential vulnerability to climate warming and human-related water uses. The two approaches presented here can be applied with a variety of other continuous phenomena to address historical changes, extreme events, and their associated ecological responses.

Keywords: frequency analyses, probability distributions, kurtosis, skew, global warming, stream ecosystems, hydrology, thermal regimes

INTRODUCTION

Environmental fluctuation is a fundamental feature that shapes ecological and evolutionary processes. Although empirical distributions of environmental data can be characterized in terms of the central tendency (or location), dispersion, and shape, most traditional statistical approaches are based on detecting changes in location and dispersion, and tend to oversimplify assumptions about temporal variation and shape. This issue is particularly troublesome for understanding the stationarity of temporally continuous phenomena and thus, the detection of potential shifts in distributional properties beyond the location and dispersion. For instance, descriptors of location, such as mean, median or mode, may not be the most informative when extreme hydrological events are of primary attention (e.g., Chebana et al., 2012). In many regions, the future climate is expected to be characterized by increasing the frequency of extreme events (e.g., Jentsch et al., 2007; IPCC 2012). Hence, the detection of changes in the shape of empirical distributions could be more informative than only using traditional descriptors of central tendency and dispersion (e.g., Shen et al., 2011; Donat & Alexander, 2012). More importantly, factors associated with changes in the shape of empirical distributions may have greater effects on species and ecosystems than do simple changes in location and dispersion (e.g., Colwell, 1974; Gaines & Denny, 1993; Thompson et al., 2013; Vasseur et al., 2014).

Here, we explore two approaches that identify and visualize temporal alterations in continuous environmental variables using thermal regimes of streams as an illustrative example. First, applying frequency analysis, we examine patterns of variability and long-term shifts in the shape of the empirical distribution of stream temperature using higher-order statistical moments (skewness and kurtosis) by season across decades. Second, we combine non-metric multidimensional scale ordination technique (N-MDS) and highest density regions (HDR) plots to detect potentially anomalous years. To exemplify the utility of these approaches, we employ them to evaluate predictions about long-term responses of thermal regimes of streams to changing terrestrial climates and other human-related water uses (Fig. 1). Our main goal is to identify temporal changes of environmental regimes not captured by lower-order statistical moments. This is particularly relevant in streams because (1) global environmental change may affect water quality beyond the traditional lower-order statistical moments (e.g., Brock & Carpenter, 2012), and (2) ecosystems and organisms have been shown to be sensitive to such changes (e.g., Thompson et al., 2013; Vasseur et al., 2014).

Thermal regime of streams as an illustrative example

Temperature is a fundamental driver of ecosystem processes in freshwaters (Shelford, 1931; Fry, 1947; Magnuson et al., 1979; Vannote & Sweeney, 1980). Short-term (daily/weekly/monthly) descriptors of mean and maximum temperatures during summertime are frequently used for characterizations of thermal habitat availability and quality (McCullough et al., 2009), definitions of regulatory thresholds (Groom et al., 2011), and predictions about possible influences of climate change on streams (Mohseni et al., 2003; Mantua et al., 2010; Arismendi et al., 2013a,b). These simple descriptors can serve as useful first approximations, but do not capture the full range of thermal conditions that the aquatic biota experience at daily, seasonal, or annual intervals (see Poole & Berman, 2001; Webb et al., 2008). Both human impacts and climate change have been shown to affect thermal regimes of streams at a variety of temporal scales (e.g., Steel & Lange, 2007; Arismendi et al., 2012; 2013a,b). For example, recent climate warming could lead to different responses of streams that may not be well described using average or maximum temperature values (Arismendi et al., 2012). Daily minimum stream temperatures in winter have warmed faster than daily maximum values during summer (Arismendi et al., 2013a; for air temperatures see Donat & Alexander, 2012). In human modified streams, seasonal shifts in stream temperatures and earlier warmer temperatures have been recorded following removal of riparian vegetation (Johnson & Jones, 2000). Simple threshold descriptors of central tendency (location) and dispersion cannot characterize these shifts.

Using higher-order statistical moments, we examine the question of whether the warming climate has led shifts in the distribution of stream temperatures (Fig. 1a, b) or if all stream temperatures have warmed similarly and moved without any change in distribution or shape. In addition, we compare these potential shifts in the distribution of stream temperature between streams with unregulated and human-regulated streamflows. Using a technique that combines a non-metric multidimensional scaling procedure and higher density region plots, we address the question of whether potentially anomalous years are synoptically detected across streams types (regulated and unregulated) and examine if those potentially anomalous years represent the influence of regional climate or alternatively highlight the importance of local factors. Previous studies have shown that detecting changes in thermal regimes of streams is complex and the use of only traditional statistical approaches may oversimplify characterization of a variety of responses of ecological relevance (Arismendi et al., 2013a,b).

MATERIAL AND METHODS

Study sites and time series

We selected long-term gage stations (US Geological Survey and US Forest Service) that monitored year-round daily stream temperature in Oregon, California, and Idaho (*n* = 10; Table 1). The sites were chosen based on (1) availability of continuous daily records for at least 31 years (January 1st 1979 to December 31st 2009) and (2) complete information for time series of daily minimum (min), mean (mean), and maximum (max) stream temperature for at least 93% of the period of record. Half of the sites (n = 5) were located in unregulated streams (sites 1-5) and the other half were in regulated streams (sites 6-10). Regulated streams were those with reservoirs constructed before 1978, whereas unregulated streams had no reservoirs upstream during the entire time period of the study (1979-2009). Time series were carefully inspected and the percentage of daily missing records of each time series was less than 7% (Table 1). To ensure enough observations to adequately represent the tails of the respective distributions at a seasonal scale for analyses of higher-order statistical moments (i.e., winter: December-February; spring: March-May; summer: June-August; fall: September-November), we grouped and compared daily stream temperature data at each site among the three decades 1980-1989, 1990-1999, and 2000-2009. For the procedure that detects potentially anomalous years only (see below), we interpolated missing data following Arismendi et al. (2013a).

Higher-order statistical moments

To visualize and use a similar scale of stream temperatures across sites, we standardized time series of daily temperature values using a Z-transformation as follows:

$$ST_i = \frac{T_i - \mu}{\sigma}$$

where ST_i was the standardized temperature at day i, T_i was the actual temperature value at day i (°C), μ was the mean and σ was the standard deviation of the respective time series considering the entire time period.

Although common estimators of skewness and kurtosis are unbiased only for normal distributions, these moments can be useful to describe changes in the shape of the distribution of environmental variables over long-term periods (see Shen et al., 2011; Donat & Alexander, 2012). Skewness addresses the question of whether or not a certain variable is symmetrically distributed around its mean value. With respect to temperature, positive skewness of the distribution (or skewed right) indicates colder conditions are more common (Fig. 1a) whereas negative skewness (skewed left) represents increasing prevalence of warmer conditions (Fig. 1b). Therefore, increases in the skewness over time could occur with increases in warm conditions, decreases in cold conditions, or both.

Kurtosis describes the structure of the distribution between the center and the tails representing the dispersion around its 'shoulders'. In other words, as the probability mass decreases around its shoulders it may increase in either the center, or the tails, or both resulting in a rise in the peakedness, the tailweight, or both and thus, the dispersion of the distribution around its shoulders increases. The reference standard is zero, a normal distribution with excess kurtosis equal to kurtosis minus three (mesokurtic). A sharp peak in a distribution that is more extreme than a normal distribution (excess kurtosis exceeding zero) is represented by less dispersion in the observations over the tails (leptokurtic). Distributions with higher kurtosis tend to have "tails" that are more accentuated. Therefore, observations are spread more evenly throughout the tails. A distribution with tails more flattened than the normal distribution (excess kurtosis below zero) is described by higher frequencies spread across the tails (platykurtic). With respect to temperature, a leptokurtic distribution may indicate that average conditions are much more frequent with a lower proportion of both extreme cold and warm values (Fig. 1a). A platykurtic distribution represents a more evenly distributed distribution across all values with a higher proportion of both extreme cold and warm values (Fig. 1b). Therefore, increases in the kurtosis over time would occur with decreases in extreme conditions, increases of average conditions, or both.

Time series of environmental data are generally large datasets that often have missing values and errors (see Table 1). Although the data we selected had no more than 7% missing values, we accounted for potential bias inherent to incomplete time series or small samples sizes by using sample skewness (adjusted Fisher-Pearson standardized moment coefficient) and sample excess kurtosis (Joanes and Gill, 1998). The sample skewness and sample excess kurtosis are dimensionless and were estimated as follows:

$$Skewness = \frac{n}{(n-1)(n-2)}\sum_{i=1}^{n}\left(\frac{T_i-\mu}{\sigma}\right)^3$$

$$Kurtosis = \left[\frac{n(n+1)}{(n-1)(n-2)(n-3)}\sum_{i=1}^{n}\left(\frac{T_i-\mu}{\sigma}\right)^4\right] - \frac{3(n-1)^2}{(n-2)(n-3)}$$

where n represented the number of records of the time series, T_i was the temperature of the day i, μ and σ the mean and standard deviation of the time series.

To define the status of the skewness for the stream temperature distribution in a particular season and decade, we followed Bulmer (1979) in defining three categories as follows: “highly skewed” (if skewness was < -1 or > 1), “moderately skewed” (if skewness was between -1 and -0.5 or between 0.5 and 1), and “symmetric” (if skewness was between -0.5 and 0.5). We used similar procedures to define the status of excess kurtosis. We defined five categories that included “negative kurtosis or platykurtic” (if kurtosis was < -1), “moderately platykurtic” (if kurtosis was between -0.5 and -1), “positive kurtosis or leptokurtic” (if kurtosis was > 1), "moderately leptokurtic" (if kurtosis was between 0.5 and 1). Finally, if kurtosis was between -0.5 and 0.5, we considered the distribution as "mesokurtic".

There are some caveats inherent to time series analyses of environmental data that should be considered. First, error terms for sequential time periods may be influenced by serial correlation affecting the independence of data. For hypothesis testing, when serial correlation occurs, the goodness of fit is inflated and the estimated standard error is smaller than the true standard error. Serial correlation often occurs on short-term scales (hourly, daily, weekly) in analyses of environmental water quality (Helsel & Hirsch, 1992). In this study, we reduced the potential for serial correlation by using higher-order statistical moments aggregated over longer time periods that allowed for a contrast among decades. Second, it is important to note that temporal changes in skewness and kurtosis could be influenced by several factors. Because skewness and kurtosis are ratios based on lower-order moments, their temporal changes may be the result of changes in only the lower-order moments, changes in the higher-order moments or both. Thus, we recommend the use of higher-moment ratios in conjunction to the lower-order moments of central tendency and dispersion.

Statistical procedure to detect potentially anomalous years

We considered an entire year as one finite-dimensional observation (365 days of daily minimum stream temperature; see s*tudy sites and time series* section above). Using a non-metric multidimensional scaling (N-MDS) unconstrained ordination technique (Kruskal, 1964), we compared the similarity among years of the Euclidean distance of standardized temperatures for each day within a year across all years. The N-MDS analysis places each year in multivariate space in the most parsimonious arrangement (relative to each other) with no a priori hypotheses.

Based on an iterative optimization procedure, we minimized a measure of disagreement or stress between their distances in 2-D using 999 random starts following the original MDSCAL algorithm (Kruskal, 1964; Clarke, 1993; Clarke & Gorley, 2006). The algorithm started with a random 2-D ordination of the years and it regressed the inter-year 2-D distances to the actual multidimensional distances (365-D). The distance between the *j*th and the *k*th year of the random 2-D ordination is denoted as d_{jk} whereas the corresponding multidimensional distance is denoted as *Djk*. The algorithm performed a non-parametric rank order regression using all the *j*th and the *k*th pairs of values. The goodness of fit of the regression was estimated using the Kruskal's stress as follows:

$$Stress = \sqrt{\frac{\sum_j \sum_k \left(d_{jk} - \hat{d}_{jk}\right)^2}{\sum_j \sum_k d_{jk}^2}}$$

where $\hat{d}_{jk}$ represented the predicted distance from the fitted regression between d_{jk} and *Djk*. If $d_{jk} = \hat{d}_{jk}$ for all the distances, the stress is zero. The algorithm used a steepest descent numerical optimization method to evaluate the stress of the proposed ordination and it stops when the stress converges to a minimum. Clarke (1993) suggests the following benchmarks: stress <0.05 – excellent ordination; stress <0.1 - good ordination; stress <0.2 acceptable ordination; stress >0.2 – poor ordination. The resulting coordinates 1 and 2 from the resulted optimized 2-D plot provided a collective index of how unique a given year was (Fig. 1c,d). In N-MDS the order of the axes was arbitrary and the coordinates represented no meaningful absolute scales for the axis. Fundamental to this method was the relative distances between points; those with greater proximity indicated a higher degree of similarity, whereas more dissimilar points were positioned further apart. We performed the N-MDS analyses using the software Primer ver. 6.1.15 (Clarke, 1993; Clarke & Gorley, 2006).

We created a bivariate high dimensional region (HDR) box-plot using the two coordinates of each point (year) from the 2-D plot from the N-MDS ordination (Hyndman, 1996). The HDR plot has been typically produced using the two main principal component scores from a traditional principal component analysis (PCA) (Hyndman, 1996; Chebana et al., 2012). However, in this study, we modified this procedure taking the advantage of the higher flexibility and lack of assumptions of the N-MDS analysis (Everitt, 1978; Kenkel & Orloci, 1986) to provide the two coordinates needed to create the HDR plot. In the HDR plot, there are regions defined based on a probability coverage (e.g., 50%; 90%; or 95%) where all points (years) within the probability coverage region have higher density estimates than any of the points outside the region (Fig. 1c,d). The outer-region of the probability coverage region (Fig. 1c,d) is bounded by points representing potentially anomalous years. We created the HDR plots using the package 'hdrcde' (Hyndman et al., 2012) in R ver. 2.15.1 (R Development Core Team, 2012).

Similarly to the higher-order statistical moments, there are some caveats that should be considered when using the procedure that detect potentially anomalous years. First, it is important to note that this procedure identified years outside a confidence region, in other words, those years that fall in the tails of the distribution. Because the confidence region represented an overall pattern extracted from the available data, it was constrained by the length of the time series. Thus, potentially anomalous years located outside of the confidence region may not necessarily represent true outliers. In addition, when the ordination is poor (stress > 0.2) interpreting the regularity/irregularity of the geometry of the confidence region should be done with caution. In our illustrative example, the regularity of the confidence region seen for regulated streams (Fig. 1c), when contrasted to unregulated sites, could be interpreted as influence of the reservoir in dampening the inter-annual variability of downstream water temperature.

RESULTS AND DISCUSSION

Empirical distributions of stream temperature were distinctive among seasons, and seasons were relatively similar across sites (Fig. 2). Temperature distributions during winter had high overlap with those during spring. Winter had the narrowest range and, as would be expected, the highest frequency of observations occurring at colder standardized temperature categories (-1.3, -0.7). The second highest proportion of observations occurred in different seasons for regulated and unregulated sites; during spring in unregulated streams and during summer at four of the five regulated sites. This shift of frequency could be due to warming and release of the warmer water from the upstream reservoirs. Fall distributions showed broadest range, with a similar proportion for a number temperature values.

Changes in the shape of empirical distributions among seasons over decades were not immediately evident. However, the values of skewness or types of kurtosis captured these decadal changes in cases when lower-order statistical moments (average and standard deviation) did not show marked differences (e.g., site1 during fall and spring in Fig. 3; Table 2 and 3; see also differences among decades at site1 during summer in Supplement). The utility of combining skewness and kurtosis to detect changes in distributional shapes over time can be illustrated using site3 during winter and spring (Tables 2 and 3; Supplement). At this site, there was a shift across decades from symmetric towards a negatively skewed distribution in winter and from symmetric towards positively skewed in spring (Table 2), as well as from mesokurtic towards a leptokurtic distribution in both winter and spring (Table 3). Overall, in most unregulated sites, kurtosis type differed among decades s during winter and summer (Table 3; Supplement). Winter and summer frequently had negatively skewed distributions whereas spring generally had positively skewed distributions or those with little change across decades, except for site3 (Table 2; Supplement).

Decadal changes in both skewness and kurtosis during winter and summer at unregulated sites suggest that the probability mass moved from its shoulders into warmer values at its center, but maintained the tail-weight of the extreme cold temperature values (Fig. 3; Tables 2 and 3; Supplement). However, in spring the probability mass diminished around its shoulders, likely due to decreases in the frequency of extreme cold temperature values. Hence, higher-order statistical moments may help in describing the complexity of temporal changes in stream temperature among seasons and highlight how shifts may occur at different portions of the distribution (e.g., extreme cold, average, or warm conditions) or among streams.

In regulated sites, we observed shifts toward colder temperatures (e.g., site6 and site9 during summer and fall in Fig. 3; Supplement) suggesting local influences of water regulation may dominate the impacts from warming climate. This is illustrated by the mixed patterns of skewness and kurtosis due to climate and water regulation, especially during spring, winter, and summer (Tables 2 and 3; Fig. 3; Supplement). In particular, in spring, patterns of skewness in regulated sites were similar to unregulated sites, whereas patterns of kurtosis were in opposite directions (more platykurtic in regulated sites). This can be explained by the water discharged from reservoirs in spring that could be a mix of the cool inflows to the reservoir, the deep, colder water stored in the reservoir over the winter, and the accelerated warming of the exposed surface of the reservoir. Patterns of skewness and kurtosis seen in regulated sites also highlight the influences of site-dependent water management coupled with climatic influences. This is exemplified by the skewness of site7 and site8 compared to site9 and site10 in fall, winter, and spring (Table 2) and the high variability of the value of skewness among sites in summer.

Increased understanding of the shape of empirical distributions by season or by year will help researchers and resource managers evaluate potential impacts of shifting environmental regimes on organisms and processes across a range of disturbance types. Empirical distributions are a simple, but comprehensive way to examine high frequency measurements that include the full range of values. Higher-order statistical moments provide useful information to characterize and compare environmental regimes and can show which seasons are most responsive to disturbances. The use of higher-order moments could help improve predictive models of climate change impacts in streams by incorporating full environmental regimes into scenarios rather than only using descriptors of central tendency and dispersion from summertime.

The technique for detection of potentially anomalous years used here was able to incorporate all daily data to provide a simple but comprehensive comparison of environmental regimes among years. We were able to characterize whole year responses and identify where regional climatic or hydrologic trends dominated versus where local influences distinctively influenced stream temperature. For example, Year 1992 was identified as potentially anomalous at three unregulated sites (or four at 90% CI) and at two regulated sites (or four at 90% CI), and identified that across the region, the majority of stream temperatures were being influenced. Stream temperatures in Years 1987 and 2008 were less synchronous across the region, but regulated and unregulated sites located in the same watershed (site2, site7, and site8 in Table 1; Figs. 4 and 5; Supplement) shared similar potentially anomalous years. We also observed site specific anomalous years, suggesting that more local conditions of watersheds influenced stream temperature (e.g., Arismendi et al., 2012). Indeed, sites located close to one another (site3 and site4 in Table 1; Fig. 4; Supplement) did not necessarily share all potentially anomalous years, suggesting that local drivers were more influential than regional climate forces during those years. Hence, the procedure for detection of potentially anomalous years used here may be useful to evaluate and contrast the vulnerability of streams to regional or local climate changes by characterizing years with anomalous conditions.

The technique that detects potentially anomalous years identified years with differences in either magnitude or timing of events (Figs. 4 and 5) and mapped these differences within the ordination plot. For example, year 1992 and 1987 were potentially anomalous likely due to magnitude of warming throughout year. At other sites, such as site3, site4 and site5 (Fig. 4), the potentially anomalous years were most likely due to increased temperatures in seasons other than summertime, and not related to higher summertime temperatures. Years 1992 and 2008 plotted at the opposite extremes of the ordination plot for site1, site2 and site7 (Figs. 4 and 5); see also Years 1982-1983 and 1986-1987 for site3. These years contained warm and cold conditions, respectively, and likely influenced the shape of the confidence region (Figs. 4 and 5; Supplement). Interestingly, we observed that the confidence region for unregulated sites (Fig. 4) appeared to be more irregularly shaped than regulated sites (Fig. 5), which suggests that stream regulation may tightly cluster and homogenize temperature values across years (e.g., Fig. 1c, d). Further attention on the interpretation of the geometry of confidence region may be useful to contrast purely climatic from human influences on streams.

There are some considerations when detecting potential changes in continuous environmental phenomena that are inherent to time series analysis including the length, timing, and quality of the time series as well as the type of the driver that is investigated as responsible for such change. Often, the detection of shifts in time series of environmental data is affected by the amount of censored data that limits the length and timing of the time series (e.g., Arismendi et al. 2012). There are uncertainties regarding the importance of regional drivers and the representativeness of sites (e.g., complex mountain terrain) and periods of record (e.g., ENSO, and PDO climatic oscillations). Lastly, the type of climatic influences may affect the magnitude and duration of the responses resulting in short-term abrupt shifts (e.g., extreme climatic events), persistent long-term shifts (e.g., climate change), or a more complex combination of them (e.g., regime shifts - Brock & Carpenter, 2012).

SUMMARY AND CONCLUSIONS

Here we show the utility of using higher-order statistical moments and a procedure that detects potentially anomalous years as complementary approaches to identify temporal changes in environmental regimes and evaluate whether these changes are consistent across years and sites. Stream ecosystems are exposed to multiple climatic and non-climatic forces which may differentially affect their hydrological regimes (e.g., temperature and streamflow). In particular, we show that potential timing and magnitude of responses of stream temperature to recent climate warming and other human-related impacts may vary among seasons, years, and across sites. Statistics of central tendency and dispersion may or may not distinguish between thermal regimes or characterize changes to thermal regimes, which could be relevant to understanding their ecological and management implications. In addition, when only single metrics are used to describe environmental regimes, they have to be selected carefully. Often selection means simplification resulting in the compression or loss of information (e.g., Arismendi et al., 2013a). By examining the whole empirical distribution and multiple moments, we can provide a better characterization of shifts over time or following disturbances than simple thresholds or descriptors.

In conclusion, our two approaches complement traditional summary statistics by helping to characterize continuous environmental regimes across seasons and years, which we illustrate using stream temperatures in unregulated and regulated sites as an example. Although we did not include a broad range of stream types, they were sufficiently different to demonstrate the utility of the two approaches. These two approaches are transferable to many types of continuous environmental variables and regions and suitable for examining seasonal and annual responses as well as climate or human-related influences (e.g., for streamflow see Chebana et al., 2012; for air temperature see Shen et al., 2011). These analyses will be useful to characterize the strength of the resilience of regimes and to identify how regimes of continuous phenomena have changed in the past and may respond in the future.

ACKNOWLEDGEMENTS

Brooke Penaluna and two anonymous reviewers provided comments that improved the manuscript. Vicente Monleon revised statistical concepts. Part of the data was provided by the HJ Andrews Experimental Forest research program, funded by the National Science Foundation's Long-Term Ecological Research Program (DEB 08-23380), US Forest Service Pacific Northwest Research Station, and Oregon State University. Financial support for IA was provided by US Geological Survey, the US Forest Service Pacific Northwest Research Station and Oregon State University through joint venture agreement 10-JV-11261991-055. Use of firm or trade names is for reader information only and does not imply endorsement of any product or service by the U.S. Government.

REFERENCES

Arismendi I, Johnson SL, Dunham JB, Haggerty R, Hockman-Wert D (2012) The paradox of cooling streams in a warming world: Regional climate trends do not parallel variable local trends in stream temperature in the Pacific continental United States. *Geophysical Research Letters*, 39, L10401.

Arismendi I, Johnson SL, Dunham JB, Haggerty R (2013a) Descriptors of natural thermal regimes in streams and their responsiveness to change in the Pacific Northwest of North America. *Freshwater Biology*, 58, 880-894.

Arismendi I, Safeeq M, Johnson SL, Dunham JB, Haggerty R (2013b) Increasing synchrony of high temperature and low flow in western North American streams: double trouble for coldwater biota? *Hydrobiologia*, 712, 61-70.

Brock WA, Carpenter SR (2012) Early warnings of regime shift when the ecosystem structure is unknown. *PLoS ONE*, 7, e45586.

Bulmer MG (1979) Principles of Statistics. Dover Publications Inc., New York.

Chebana F, Dabo-Niang S, Ouarda TBMJ (2012) Exploratory functional flood frequency analysis and outlier detection. *Water Resources Research*, 48, W04514.

Clarke KR (1993) Nonparametric multivariate analyses of changes in community structure. *Australian Journal of Ecology*, 18, 117-143.

Clarke KR, Gorley RN (2006) PRIMER v6: User Manual/Tutorial. PRIMER-E, Plymouth.

Colwell RK (1974) Predictability, constancy, and contingency of periodic phenomena. *Ecology*, 55, 1148-1153.

Donat MG, Alexander LV (2012) The shifting probability distribution of global daytime and night-time temperatures. *Geophysical Research Letters*, 39, L14707.

Everitt B (1978) *Graphical techniques for multivariate data*. North-Holland, New York.

Fry FEJ (1947) *Effects of the environment on animal activity*. University of Toronto Studies, Biological Series 55. Publication of the Ontario Fisheries Research Laboratory, 68, 1-62.

Gaines SD, Denny MW (1993) The largest, smallest, highest, lowest, longest, and shortest: extremes in ecology. *Ecology*, 74, 1677–1692.

Groom JD, Dent L, Madsen LJ, Fleuret J (2011) Response of western Oregon (USA) stream temperatures to contemporary forest management. *Forest Ecology and Management*, 262, 1618-1629.

Helsel DR, Hirsch RM (1992) Statistical methods in water resources, Elsevier, Netherlands.

Hyndman RJ (1996) Computing and graphing highest density regions. *The American Statistician*, 50, 120-126.

Hyndman RJ, Einbeck J, Wand M (2012) *Package 'hdrcde': highest density regions and conditional density estimation.* http://cran.r-project.org/web/packages/hdrcde/hdrcde.pdf

IPCC (2012) Managing the risks of extreme events and disasters to advance climate change adaptation. In: A Special Report of Working Groups I and II of the Intergovernmental Panel on Climate Change (eds Field CB, Barros V, Stocker TF, Qin D, Dokken DJ, Ebi KL, Mastrandrea MD, Mach KJ, Plattner GK, Allen SK, Tignor M, Midgley PM). Cambridge University Press, Cambridge, United Kingdom and New York, NY, USA, pp. 1-19.

Jentsch A, Kreyling J, Beierkuhnlein C (2007) A new generation of climate change experiments: events, not trends. *Frontiers in Ecology and Environment*, 5, 365-374.

Joanes DN, Gill CA (1998) Comparing measures of sample skewness and kurtosis. *Journal of the Royal Statistical Society (Series D): The Statistician*, 47, 183-189.

Johnson SL, Jones JA (2000) Stream temperature response to forest harvest and debris flows in western Cascades, Oregon. *Canadian Journal of Fisheries and Aquatic Sciences*, 57, 30-39.

Kruskal JB (1964) Non-metric multidimensional scaling: a numerical method. *Psychometrika*, 29, 115-129.

Kenkel NC, Orloci L (1986) Applying metric and nonmetric multidimensional scaling to ecological studies: some new results. *Ecology*, 67, 919-928.

Magnuson JJ, Crowder LB, Medvick PA (1979) Temperature as an ecological resource. *American Zoologist*, 19, 331-343.

Mantua N, Tohver I, Hamlet A (2010) Climate change impacts on streamflow extremes and summertime stream temperature and their possible consequences for freshwater salmon habitat in Washington State. *Climatic Change*, 102, 187-223.

McCullough DA, Bartholow JM, Jager HI *et al*. (2009) Research in Thermal Biology: Burning Questions for Coldwater Stream Fishes. *Reviews in Fisheries Science*, 17, 90-115.

Mohseni O, Stefan HG, Eaton JG (2003) Global warming and potential changes in fish habitat in U.S. streams. *Climatic Change*, 59, 389-409.

Poole GC, Berman CH (2001) An ecological perspective on in-stream temperature: natural heat dynamics and mechanisms of human-caused thermal degradation. *Environmental Management*, 27, 787-802.

Thompson RM, Beardall J, Beringer J, Grace M, Sardina P (2013) Means and extremes: building variability into community-level climate change experiments. *Ecology Letters*, 16, 799-806.

Shelford VE (1931) Some concepts of bioecology. *Ecology*, 123, 455-467.

Shen SSP, Gurung AB, Oh H, Shu T, Easterling DR (2011) The twentieth century contiguous US temperature changes indicated by daily data and higher statistical moments. *Climatic Change*, 109, 287-317.

Steel EA, Lange IA (2007) Using wavelet analysis to detect changes in water temperature regimes at multiple scales: effects of multi-purpose dams in the Willamette River basin. *River Research Applications*, 23, 351-359.

Vannote RL, Sweeney BW (1980) Geographic analysis of thermal equilibria: a conceptual model for evaluating the effects of natural and modified thermal regimes on aquatic insect communities. *American Naturalist*, 115, 667-695.

Vasseur DA, DeLong JP, Gilbert B, Greig HS, Harley CDG, McCann KS, Savage V, Tunney TD, O’Connor MI (2014) Increased temperature variation poses a greater risk to species than climate warming. *Proceedings of the Royal Society B*, 281, 20132612.

Webb BW, Hannah DM, Moore RD, Brown LE, Nobilis F (2008) Recent advances in stream and river temperature research. *Hydrological Processes*, 22, 902-918.

SUPPORTING INFORMATION

Supplement Supplementary results of skewness, kurtosis, and outlier’s detection

Table 1. Location and characteristics of unregulated (n = 5) and regulated (n = 5) streams at the gaging sites. Percent of daily gaps in the stream temperature time series from Jan-1979 to Dec-2009 used in this study.

River	**Start of water regulation**	**gage ID**	**ID**	**Lat N**	**Long W**	**elevation (m)**	**watershed area (km^2)**	**% of daily gaps**
Fir Creek, OR	unregulated	14138870	site1	45.48	122.02	439	14.1	2.8%
SF Bull Run River, OR	unregulated	14139800	site2	45.45	122.11	302	39.9	2.0%
McRae Creek, OR	unregulated	TSMCRA	site3	44.26	122.17	840	5.9	3.5%
Lookout Creek, OR	unregulated	TSLOOK	site4	44.23	122.12	998	4.9	2.6%
Elk Creek, OR	unregulated	14338000	site5	42.68	122.74	455	334.1	5.2%
Clearwater River, ID	1971	13341050	site6	46.50	116.39	283	20,658	4.0%
Bull Run River near Multnomah Falls, OR	1915[a]	14138850	site7	45.50	122.01	329	124.1	5.3%
NF Bull Run River, OR	1958	14138900	site8	45.49	122.04	323	21.6	2.6%
Rogue River near McLeod, OR	1977	14337600	site9	42.66	122.71	454	2,429	3.7%
Martis Creek near Truckee, CA	1971	10339400	site10	39.33	120.12	1747	103.4	6.5%

[a] Regulation at times

Table 2. Magnitude and direction of the value of skewness in probability distributions of daily minimum stream temperature by season and decade at unregulated (sites 1-5) and regulated (sites 6-10) streams. Symmetric distributions are not shown. m = moderately skewed; h = highly skewed; (-) = negatively skewed; (+) = positively skewed (see Supplement for more details).

		season/time period											
site type	**site ID**	**fall**			**winter**			**Spring**			**summer**		
		80-89	**90-99**	**00-09**	**80-89**	**90-99**	**00-09**	**80-89**	**90-99**	**00-09**	**80-89**	**90-99**	**00-09**
unregulated (1-5)	site1				m(-)	m(-)	m(-)	m(+)	m(+)	m(+)			
	site2					m(-)	m(-)	m(+)	m(+)	m(+)	m(-)		m(-)
	site3						m(-)		m(+)	h(+)			m(-)
	site4							h(+)	m(+)	h(+)	m(-)	m(-)	m(-)
	site5							m(+)	h(+)	m(+)	m(-)	m(-)	m(-)
regulated (6-10)	site6							m(+)					m(+)
	site7					m(-)		m(+)	m(+)	m(+)			m(-)
	site8	m(-)	m(-)					m(+)		m(+)			h(-)
	site9	m(+)	m(+)	m(+)	m(+)	m(+)							m(+)
	site10					m(+)					h(-)	m(-)	

Table 3. Types of kurtosis of probability distributions of daily minimum stream temperature by season and decade at unregulated and regulated sites. ↔↔ = platykurtic; ↔ = moderately platykurtic; ↕↕ = leptokurtic, and ↕ = moderately leptokurtic. Mesokurtic distributions are not shown (see Supplement for more details).

		season/time period											
site type	**site**	**fall**			**winter**			**Spring**			**summer**		
		80-89	**90-99**	**00-09**	**80-89**	**90-99**	**00-09**	**80-89**	**90-99**	**00-09**	**80-89**	**90-99**	**00-09**
unregulated (1-5)	site1			↔	↕	↕	↕	↕↕					
	site2			↔			↕	↕↕				↔	↕
	site3	↔	↔	↔			↕↕			↕	↔		
	site4			↔				↕↕		↕↕			↕
	site5	↔	↔	↔	↔				↕	↕	↕↕		↕
regulated (6-10)	site6	↔	↔	↔								↔	↕
	site7	↔		↔				↕↕					
	site8	↕		↔	↕		↕		↔			↕	↕↕
	site9			↔	↕			↔	↔	↔	↔	↔	
	site10	↔↔	↔↔	↔↔	↔	↕↕		↔↔	↔	↔	↕↕	↕	↕

FIGURE LEGENDS

Fig. 1. Conceptual diagram showing hypothesized shifts of distribution of water temperatures at both seasonal (upper panels) and annual (lower panels) scales in regulated (left panels) and unregulated (right panels) streams. In the upper panels examples of changes in skewness and kurtosis are shown for temperature distributions affected by stream regulation and a warming climate in a given season. For instance, in regulated streams the influence of the reservoir may reduce both extreme cold and warm temperatures confounding the effect from the climate (a) whereas less cold temperatures and an overall shift toward warming values may occur in unregulated streams (b). In the lower panels, we illustrate the use of N-MDS and HDR plots for detecting potentially anomalous years in regulated and unregulated streams (the shaded area represent a given coverage probability). Points located in the outer or the confidence region represent potentially anomalous years. For instance, in regulated streams individual years are more clustered due to the reservoir may homogenize temperatures across years whereas (c) whereas in unregulated streams individual years are less clustered due to more heterogeneous responses to the warming climate (b).

Fig. 2. Density plots of standardized temperatures (1979-2009) by season (winter – blue line; spring – green line; summer – red line; fall – black line) in unregulated (left panel) and regulated (right panel) streams using time series of daily minimum.

Fig. 3. Examples of (a) density plots of standardized temperatures by decade (period 80-89 dashed line; period 90-99 gray line; period 00-09 solid color line) and season using time series of daily minimum in an unregulated (site1) and a regulated (site6) stream. In the lower panel (b) central tendency statistics (average ± SD) for each decade and season (winter – blue; spring – green; summer – red; fall – black) are also included. See results for all sites in the Supplement.

Fig. 4. Bivariate HDR boxplots (left panel) and standardized daily temperature distribution (right panel) in unregulated streams using annual time series of daily minimum. The dark and light grey regions show the 50%, 90%, 95% coverage probability. The symbols outside the grey regions and darker lines represent potentially anomalous years. Examples of years between 90% and 95% of the coverage probability were italicized. See results for all sites in the Supplement.

Fig. 5. Bivariate HDR boxplots (left panel) and standardized daily temperature distribution (right panel) in regulated streams using annual time series of daily minimum. The dark and light grey regions show the 50%, 90%, 95% coverage probability. The symbols outside the grey regions and darker lines represent potentially anomalous years. Examples of years between 90% and 95% of the coverage probability were italicized. See results for all sites in the Supplement.

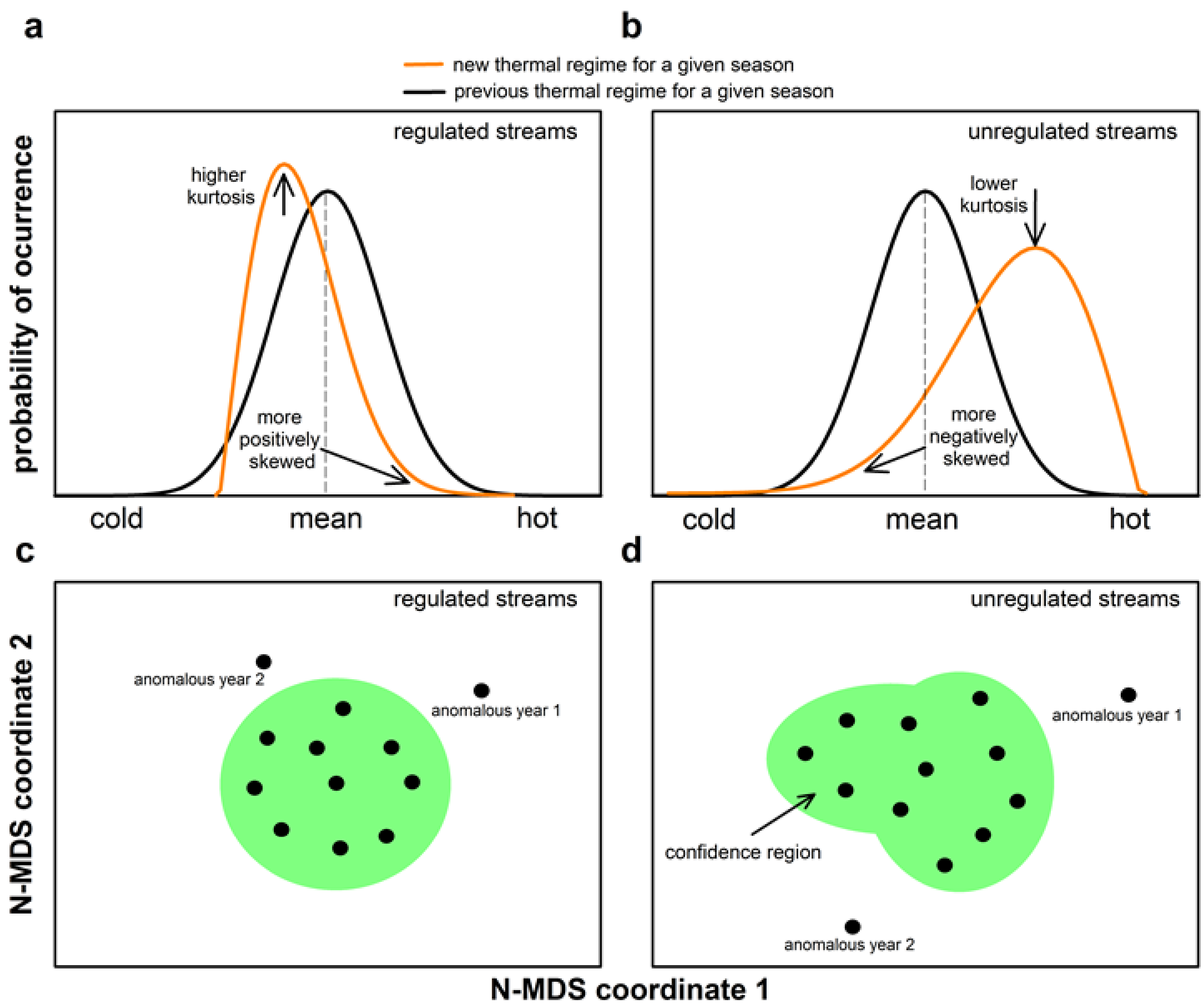
a
b
new thermal regime for a given season
previous thermal regime for a given season
regulated streams
higher kurtosis
more positively skewed
probability of ocurrence
cold
mean
hot
unregulated streams
lower kurtosis
more negatively skewed
cold
mean
hot
c
d
regulated streams
anomalous year 2
anomalous year 1
N-MDS coordinate 2
unregulated streams
anomalous year 1
confidence region
anomalous year 2
N-MDS coordinate 1

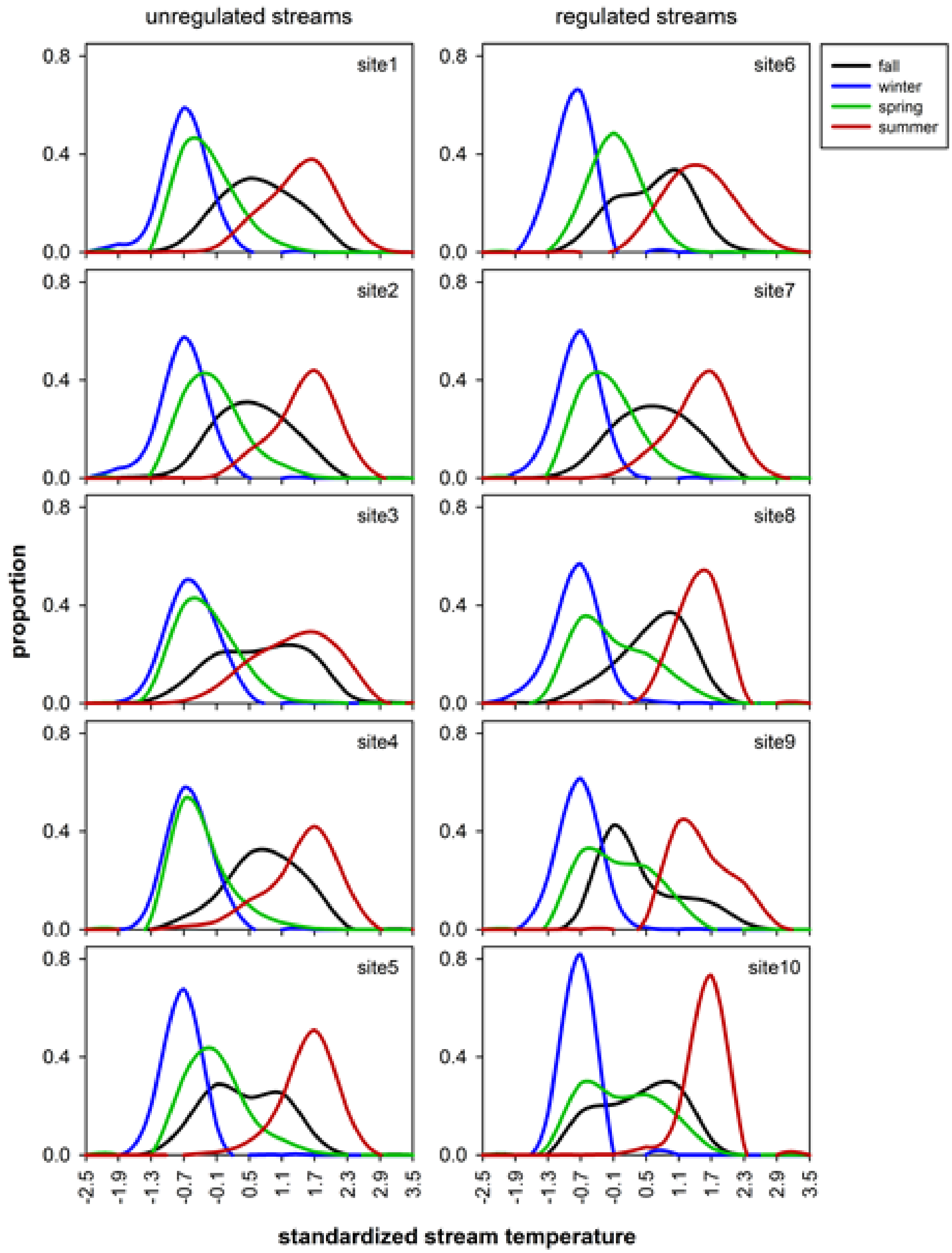

unregulated streams
regulated streams
fall
winter
spring
summer
site1
site2
site3
site4
site5
site6
site7
site8
site9
site10
proportion
0.8
0.4
0.0
-2.5
-1.9
-1.3
-0.7
-0.1
0.5
1.1
1.7
2.3
2.9
3.5
standardized stream temperature

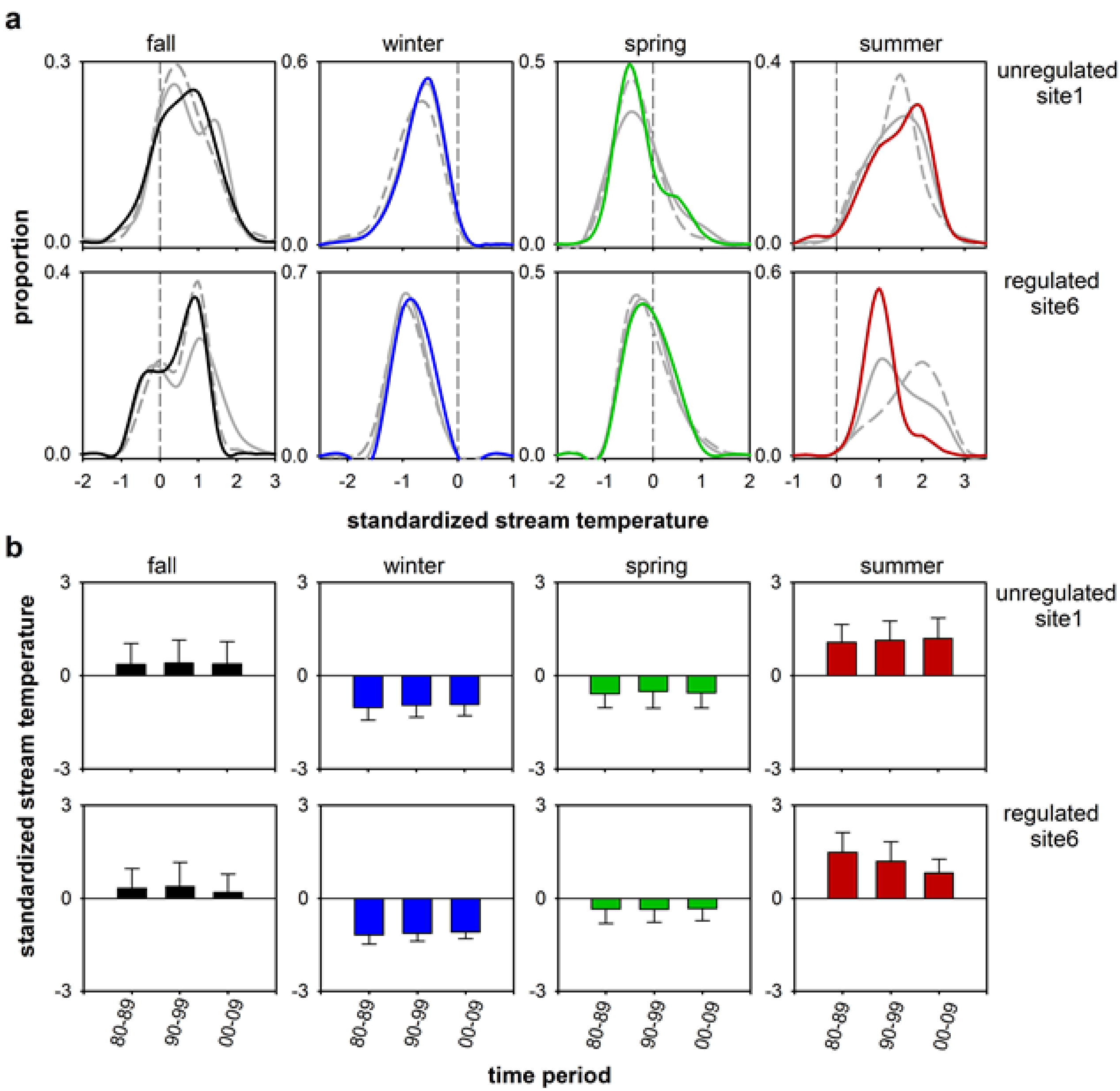
a
fall
winter
spring
summer
unregulated
site1
regulated
site6
proportion
0.3
0.0
0.6
0.0
0.5
0.0
0.4
0.0
0.4
0.0
0.7
0.0
0.5
0.0
0.6
0.0
-2 -1 0 1 2 3
-2 -1 0 1
-2 -1 0 1 2
-1 0 1 2 3
standardized stream temperature
b
fall
winter
spring
summer
unregulated
site1
regulated
site6
standardized stream temperature
3
0
-3
80-89
90-99
00-09
time period

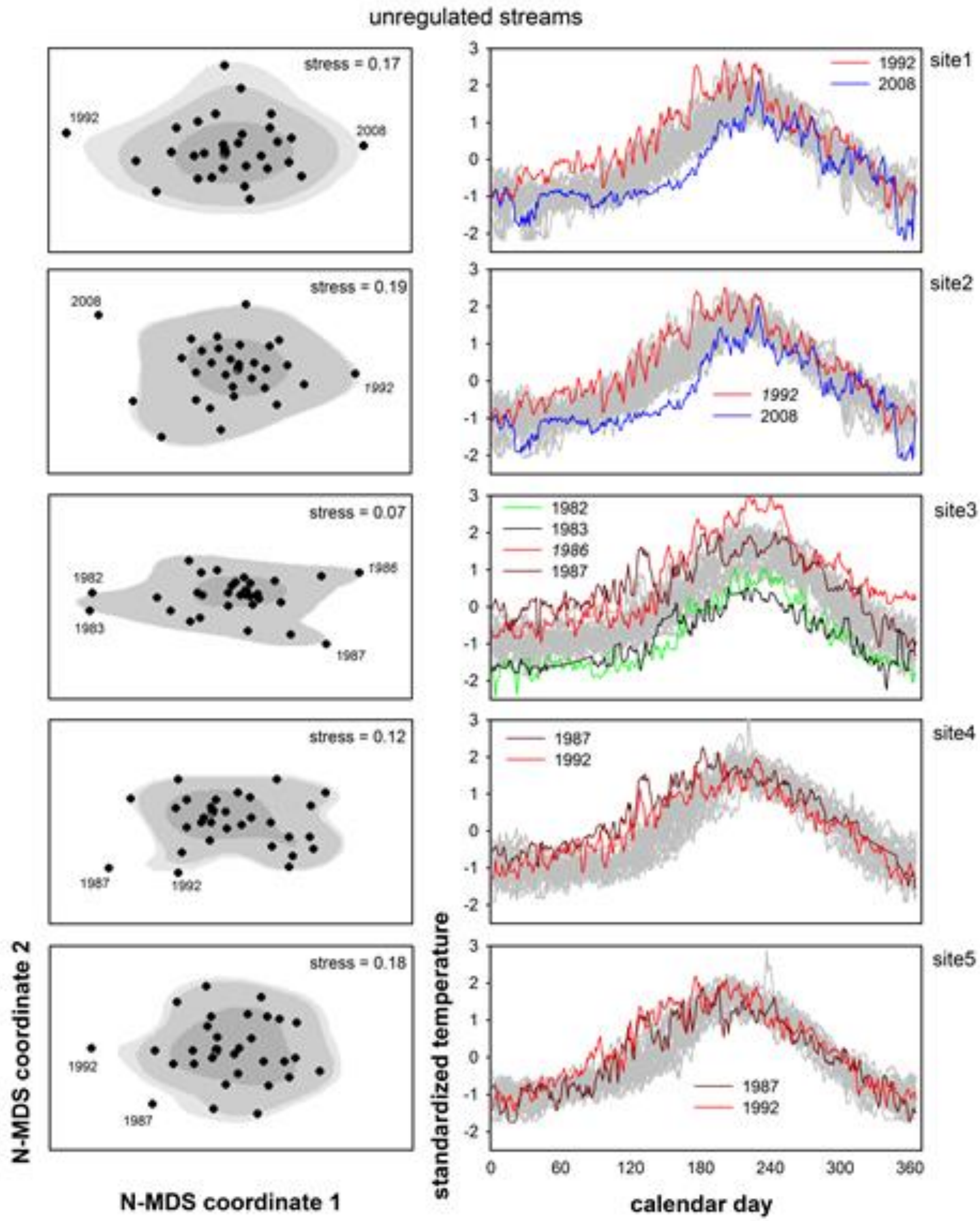
unregulated streams
stress = 0.17
1992
2008
stress = 0.19
2008
1992
stress = 0.07
1982
1983
1986
1987
stress = 0.12
1987
1992
stress = 0.18
1992
1987
N-MDS coordinate 2
N-MDS coordinate 1
site1
site2
site3
site4
site5
standardized temperature
calendar day
0
60
120
180
240
300
360
3
2
1
0
-1
-2

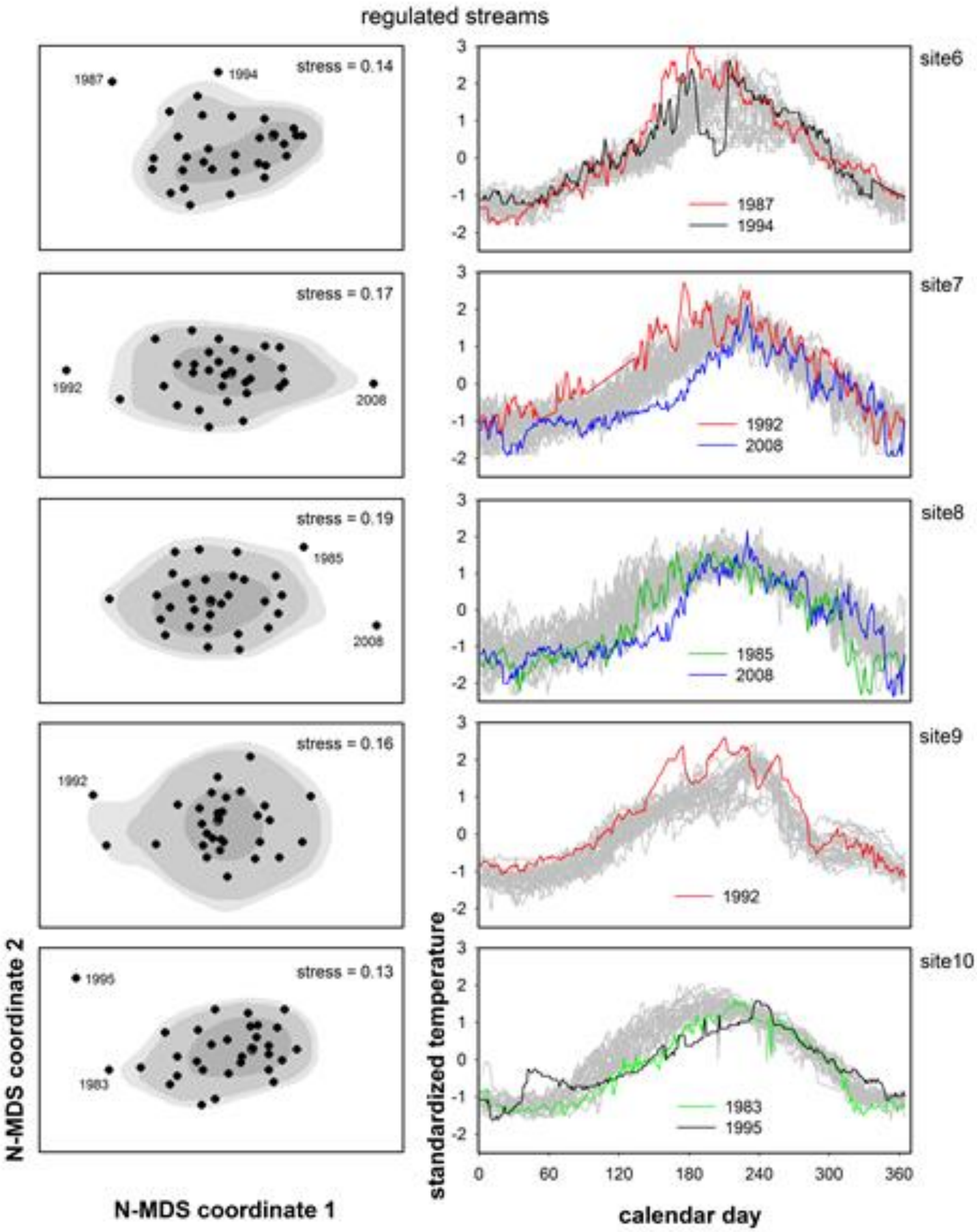
regulated streams
stress = 0.14
1987
1994
stress = 0.17
1992
2008
stress = 0.19
1985
2008
stress = 0.16
1992
stress = 0.13
1995
1983
N-MDS coordinate 2
N-MDS coordinate 1
site6
1987
1994
site7
1992
2008
site8
1985
2008
site9
1992
site10
1983
1995
standardized temperature
calendar day
0
60
120
180
240
300
360
3
2
1
0
-1
-2